

Nuclear Pseudoquadrupole Resonance of ^{141}Pr in Van Vleck Paramagnet PrF_3

E. M. Alakshin, A. S. Aleksandrov, A. V. Egorov, A. V. Klochkov,
S. L. Korableva, and M. S. Tagirov

Institute of Physics, Kazan (Volga region) Federal University, Kazan, 420008 Russia

Received May 23, 2011; in final form, June 27, 2011

Nuclear pseudoquadrupole resonance of ^{141}Pr in Van Vleck paramagnet PrF_3 has been observed in single-crystal and micro- and nanopowder samples at a temperature of 4.2 K. The spectra of nuclear pseudoquadrupole resonance of ^{141}Pr , as well as the spin–spin and spin–lattice relaxation parameters, have been obtained. The parameters of the nuclear spin Hamiltonian have been determined. It has been found that the parameters of the crystal electric field in nanocrystals differ strongly from those in microcrystals.

DOI: 10.1134/S0021364011150021

The first studies of nuclear magnetic resonance (NMR) and nuclear acoustic resonance of ^{141}Pr in Van Vleck paramagnet PrF_3 were performed as early as in 1979 [1, 2]. More recently, the magnetic coupling of praseodymium nuclei with nuclei of liquid helium-3 was studied in fine-dispersed praseodymium trifluoride [3, 4]. The NMR spectra of ^{141}Pr in PrF_3 at low temperatures are characterized by the strong anisotropy of the effective nuclear magnetic moment of praseodymium and by the presence of quadrupole and pseudoquadrupole interactions. Analyzing the NMR spectra, Bol'shakov and Teplov [1] found the parameters of the spin Hamiltonian of ^{141}Pr in PrF_3 , which are determined by the crystal electric field. They also showed that pseudoquadrupole interactions are much stronger than quadrupole interactions in this system. Pseudoquadrupole resonance has not been observed directly, i.e., in the absence of the applied static magnetic field. This is likely explained by very fast spin–spin relaxation (one line was observed in another crystal, praseodymium sulfate [5]). The NMR spectra of praseodymium in systems of disordered crystallites (powders) can be observed in almost any magnetic field due to the anisotropy of the efficient (enhanced) nuclear magnetism of praseodymium and pseudoquadrupole interaction. However, comparing this spectrum with that simulated using the known parameters, we doubt that the crystal electric fields in nanocrystals and macrocrystals are identical [6]. An analysis of nuclear pseudoquadrupole resonance of ^{141}Pr in a single crystal and powders with various degrees of dispersion makes it possible to directly measure the parameters of pseudoquadrupole Hamiltonian and to correct the parameters of the Zeeman Hamiltonian. The study of spin–spin interaction enables the estimation of the spin diffusion within the nanocrystal. In addition, we present the data on the width and lineshape of

the nuclear pseudoquadrupole resonance of ^{141}Pr in PrF_3 .

In the general case, the Hamiltonian of the rare earth ion can be represented in the form

$$H = H_{\text{CF}} + g_J \beta \mathbf{H} \mathbf{J} + a_J \mathbf{J} \mathbf{I} - \gamma_J \hbar \mathbf{H} \mathbf{I} + H_Q, \quad (1)$$

where the first term describes the interaction with the crystal electric field; the second and fourth terms correspond to the electron and nuclear Zeeman interaction, respectively; the third term describes the hyperfine interaction; and the last term is the nuclear quadrupole interaction. When the ground electronic state is a singlet (Van Vleck ion), only the ground state is occupied at temperatures that satisfy the condition $kT \ll \Delta$, where Δ is the energy of the nearest excited state. In this case, the electron nuclear levels can be calculated in the second order of perturbation theory (see, e.g., [6]). The second and third terms of Hamiltonian (1) constitute perturbation. As a result, the effective Hamiltonian that includes only nuclear spin operators can be represented in the form

$$H_I = -\hbar \sum_{\alpha=x, y, z} \gamma_{\alpha} H_{\alpha} I_{\alpha} + D \left[I_z^2 + \frac{1}{3} I(I+1) \right] + E(I_x^2 - I_y^2) + H_Q, \quad (2)$$

where γ_{α} are the components of the effective gyromagnetic ratio. The second and third terms are similar to the Hamiltonian of the nuclear quadrupole interaction. However, they are completely due to the hyperfine interaction and are independent of the quadrupole moment of the nucleus; for this reason, they are called pseudoquadrupole interaction. In the absence of magnetic field, resonance transitions are naturally called pseudoquadrupole resonance.

According to various data, the local symmetry of the Pr^{3+} ion in PrF_3 is C_s or C_2 . In the crystal field of low symmetry, the main multiplet $^3\text{H}_4$ of the Pr^{3+} ion splits into nine singlets. According to the inelastic neutron scattering data, the singlet nearest to the ground singlet is separated from the latter by 59.5 cm^{-1} [7]. According to the ^{141}Pr NMR data, the crystal contains three types of magnetically equivalent Pr^{3+} centers. The ^{141}Pr NMR spectra are described by Hamiltonian (2) with the parameters $D/h = 4.31(1) \text{ MHz}$, $E/h = 0.30(1) \text{ MHz}$, $\gamma_x/2\pi = 3.32(2) \text{ kHz/Oe}$, $\gamma_y/2\pi = 3.24(2) \text{ kHz/Oe}$, and $\gamma_z/2\pi = 10.03(5) \text{ kHz/Oe}$ [1, 2].

In those works, it was found that the quadrupole interaction can be neglected and, in the absence of magnetic field, the energy levels are only determined by the second and third terms in Hamiltonian (2). The ^{141}Pr isotope has 100% natural abundance, $I = 5/2$, and $\gamma_1/2\pi = 1.26 \text{ kHz/Oe}$. In the case of the symmetric Hamiltonian ($E = 0$), the energy levels are three doublets with the wavefunctions $|\pm 1/2\rangle$, $|\pm 3/2\rangle$, and $|\pm 5/2\rangle$. The frequencies of the allowed transitions between them are related as 1 : 2. If $E \neq 0$, the wavefunctions are mixed and the ratio of the frequencies changes. In the following the nuclear pseudoquadrupole resonance lines with lower and higher frequencies are denoted as LF and HF, respectively.

The parameters of the nuclear pseudoquadrupole resonance of ^{141}Pr were measured in three PrF_3 samples. Sample A is a single crystal grown by the Bridgeman–Stockbarger method. Sample B is a powder obtained by cleaving the single crystal in a sapphire mortar and subsequent riddling through sieves (particle size of 10–45 μm). Sample C consists of nanocrystals with a total mass of 1 g, which were synthesized by precipitation from colloidal solutions and were hydrothermally treated [8, 9]. The mean size of crystallites was 30 nm. The measurements were performed at a temperature of 4.2 K using NMR/NQR homebuilt spectrometer. The spectra are the frequency dependences of the spin echo intensity. When determining the transverse and longitudinal relaxation rates, the commonly known pulse sequences were used. Since

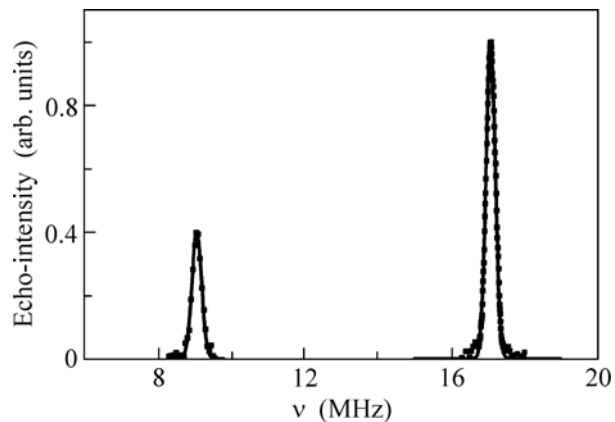


Fig. 1. Nuclear pseudoquadrupole resonance spectrum of ^{141}Pr in the PrF_3 single crystal (sample A). The solid lines are Gaussians.

the transverse relaxation rate is very high, the probe of the spectrometer was shunted so that its Q factor was not higher than 5. The minimum time interval between probe pulses at which the spin echo signal was detected was 6 μs .

Figure 1 shows the nuclear pseudoquadrupole resonance spectrum of ^{141}Pr in the PrF_3 single crystal (sample A). The shapes of the both lines are close to Gaussian. For this reason, the positions v_0 and widths Δv of the lines were determined through the Gaussian approximation. The square root of the second moment of the line is used as the width. The parameters D and E , which can be calculated knowing the transition frequencies (see table), coincide with the values obtained from the NMR spectra [1]. The lines have the same width, which indicates the dipolar broadening character. The nearest environment of Pr^{3+} consists of 11 fluorine ions. The ^{19}F nuclei have a large magnetic moment ($^{19}\gamma/2\pi = 4.007 \text{ kHz/Oe}$, $I = 1/2$). In addition to the dipolar interaction between unlike spins, the interaction between the like spins of the praseodymium nuclei contributes to the width. This contribution can only be estimated from the spin echo envelope. The observed dependences have a

Positions v_0 and width Δv of nuclear pseudoquadrupole resonances; spin–lattice, T_1 , and spin–spin, T_2 , relaxation times; and parameters D and E of spin Hamiltonian (2)

| Sample | Line | v_0 , MHz | Δv , MHz | T_1 , ms | T_2 , μs | D/h , MHz | E/h , MHz |
|--------|------|-------------|------------------|------------|-----------------------|-------------|-------------|
| A | LF | 9.063(3) | 0.134(3) | 2.3(4) | 7.3(2) | 4.311(3) | 0.314(6) |
| | HF | 17.083(1) | 0.128(1) | 10.5(8) | 10.5(2) | | |
| B | LF | 9.036(5) | 0.135(5) | 2.9(4) | 6.9(2) | 4.307(5) | 0.31(1) |
| | HF | 17.072(3) | 0.132(3) | 10.2(3) | 9.2(2) | | |
| C | LF | 9.9(1) | 2.2(2) | 2.2(9) | 10.5(2) | 4.18(4) | 0.60(4) |
| | HF | 16.15(3) | 1.60(3) | 7.3(5) | 12.7(3) | | |

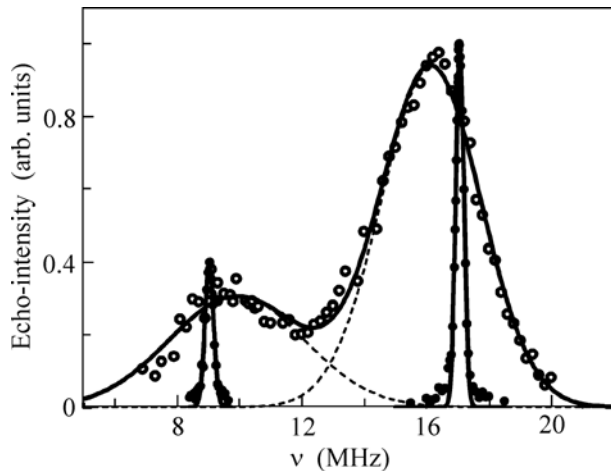


Fig. 2. Nuclear pseudoquadrupole resonance spectra of ^{141}Pr in PrF_3 (closed circles, sample B) micro- and (open circles, sample C) nanopowders. The solid lines are Gaussian approximations.

shape close to Gaussian. The data were processed with the function $\exp[-(2\tau)^2/2 T_2^2]$, where τ is the interval between the probe pulses, $T_2^{-1} = \sqrt{M_2}$, and M_2 is the second moment of the line broadened by the dipole–dipole interaction between the like spins. The line position, width T_2 , and the parameters of the spin Hamiltonian in the micropowder (sample B) are in agreement within the accuracy with the respective parameters of the single crystal (see table). Note that the high-frequency line in both samples is narrower than the low-frequency line, but this difference is close to the measurement error. This can be explained by different transverse relaxation times (different contributions to the width from the dipole–dipole interaction between the like spins T_2^{-1}). Figure 2 shows the nuclear pseudoquadrupole resonance spectra of samples B and C (nanocrystals). The ^{141}Pr spectra of the latter sample are strongly broadened and the lines are noticeably shifted. Since the shifts of the lines are large and we have no model that describes the shape of lines broadened due to the nonuniformity of the crystal electric field, the spectra were fitted by Gaussians. All of the parameters are summarized in the table. The mechanism of the spin–lattice relaxation has not yet been determined. However, for two reasons, it can be assumed that this relaxation occurs through the dipole–dipole reservoir of impurity paramagnetic ions. First, the spin–lattice relaxation time T_1 that is measured for high-frequency lines is several times longer than that for low-frequency lines. Second, the

magnetization recovers as $\exp[-(t/T_1)^{1/2}]$ (stretched exponential). It often happens in the case of relaxation through paramagnetic impurities.

It has been found that the main cause of the broadening of the nuclear pseudoquadrupole resonance lines in samples A and B is the dipole–dipole interaction with the nuclear moments of ^{19}F . The lines in sample C are broadened by a factor of more than 10, which can be explained only by the spread of the parameters of the crystal electric field. The parameters of the Hamiltonian of nuclear pseudoquadrupole interaction in sample C are noticeably different from the respective parameters for samples A and B. This can only be explained by a change in the crystal field. The transverse relaxation of ^{141}Pr in nanocrystals is insignificantly slower (see table). This indicates that the nearest spins of praseodymium remain the same and the crystal electric field varies monotonically within a nanocrystallite. The change of the mean crystal electric field parameters can occur either at a certain critical size of crystallites or gradually. To determine the real scenario, additional experiments are required.

This work was supported in part by the Ministry of Education and Science of the Russian Federation (state contract no. P900, federal program “Scientific and Pedagogical Personnel of Innovative Russia” for 2009–2013).

REFERENCES

1. I. G. Bol'shakov and M. A. Teplov, Available from VINITI, No. 1274-79 (1979).
2. S. A. Al'tshuler, A. V. Duglav, and A. Kh. Khasanov, JETP Lett. **29**, 624 (1979).
3. A. V. Egorov, D. S. Irisov, A. V. Klochkov, et al., JETP Lett. **86**, 416 (2007).
4. A. V. Egorov, D. S. Irisov, A. V. Klochkov, et al., J. Phys.: Conf. Ser. **150**, 032019 (2009).
5. F. L. Aukhadeev, V. A. Grevtsev, I. S. Konov, et al., Sov. Phys. Solid State **18**, 1228 (1976).
6. L. K. Aminov, B. Z. Malkin, and M. A. Teplov, in *Handbook on the Physics and Chemistry of Rare Earths*, Ed. by K. A. Gschneidner and L. Eyring (Elsevier, Amsterdam, 1996), Vol. 22, p. 150.
7. K. Feldmann, K. Honnig, L. P. Kaun, et al., Phys. Status Solidi B **70**, 71 (1975).
8. L. Ma, W. Chen, Y. Zheng, et al., Mater. Lett. **61**, 2765 (2007).
9. M. S. Tagirov, E. M. Alakshin, R. R. Gazizullin, et al., J. Low Temp. Phys. **162**, 645 (2011).

Translated by R. Tyapaev